Properties of pure and light antimony-doped tin oxide thin films prepared by e-beam technique

H. A. MOHAMED[a, b]
[a]Physics department, faculty of Science, Sohag University, 82524 Sohag, Egypt
[b]Physics department, Teachers College , King Saud University, 11148 Riyadh, KSA

Transparent conducting antimony-doped tin oxide SnO_2:Sb films were prepared on glass substrates by e-beam evaporation technique. The effect of Sb-content and annealing temperature on the optical, electrical and structural properties of the formed films were investigated. The as-deposited films show amorphous structure and low transmittance that increased with increasing Sb-content. Upon annealing, the film ordering increases. The annealed $(SnO2)_{100-x}Sb_x$ (x= 3 wt%) films show minimum resistivity of ~ 6×10^{-3} Ω cm at temperature 400 ^{o}C and their transmittance exceedes 84 % in the visible region. The other parameters such as free carrier concentrations, refractive index, Urbach energy were calculated for as-deposited and annealed films.

1. Introduction

Undoped tin oxide (SnO_2) is a wide band-gap semiconductors material with $E_g \sim 3.6 - 4$ eV [1-4]. SnO_2 in the form of thin film is a transparent material, characterized by high optical transmission in the visible region [5] and low resistivity. Particularly, they are stable up to high temperatures, have excellent resistance to strong acids and bases at room temperature as well as to mechanical wear and they have very good adhesion to many substrates [6]. Therefore, this material is used as transparent electrodes in many applications, such as gas sensors, solar cells, liquid crystal displays, etc [7-11]. In addition, SnO_2 films are more chemically stable than other TCOs such as zinc oxide (ZnO) and Sn-doped In_2O_3 (ITO) [12].

SnO_2 thin films can be prepared using various techniques, such as pulsed laser deposition [13], chemical vapor deposition [14], sol-gel [15] and radio-frequency magnetron sputtering [16].

It was found that the electrical resistivity of these films decreases by doping with F^- or Sb^{5+} without significant changes in their optical transmittance [17-19]. Beside, it was reported that the small amount of Sb dopant results a good electrical conductivity of SnO_2 films without losing optical transparency. However, large additions diminish the conductivity, optical transparency and crystallinity of these films [20, 21].

In this paper, the effect of small amount of Sb dopant and heat treatment on the structural, optical and electrical properties of SnO_2 thin films deposited by electron beam evaporation technique were investigated.

2. Experimental details

For preparing $(SnO_2)_{100-x}Sb_x$ (x = 0, 1, 3, 5, and 8 wt%) bulk samples, a highly pure (99.999% purity) powder of SnO_2 and Sb were ground separately and sieved. A mixture of $(SnO_2)_{100-x}Sb_x$ with different x ratio was prepared. To increase complete mixing, the mixtures were ground for at least two hours. Then, they were made into tablet form using a cold pressing technique. In order to increase the diffusion process and consequently improve the homogeneity of the material, the sintering was performed for the present mixtures at 900 $^\circ$C for 4 h.

Thin films of the considered ratios were prepared by electron beam evaporation in an Edward's high vacuum coating unit model 306 A under pressures of 5×10^{-6} Torr. The films were prepared on unheated ultrasonically cleaned microscopic glasses. The thickness of the films (≈100 nm) was controlled using a digital film thickness monitor model TM 200 Maxtek. The deposition rate was ≈10 nm/min. The post-thermal annealing of the as-deposited films was carried out in a fully controlled furnace in air for 30 min. The annealing temperature ranged from room temperature to 550 °C.

The crystallinity of the as-deposited and annealed films was examined using a Philips-PW1710 X-ray diffractometer. CuKα radiation ($\lambda = 1.541838$ Å) was used from the X-ray tube with normal focus. The optical transmittance (T) and reflectivity (R) of $(SnO_2)_{100-x}Sb_x$ films were measured using a Jasco 570 double-beam spectrophotometer over a wavelength(λ)range of 200–2500 nm at normal incidence.

The resistivity measurements were carried out using a two-terminal configuration by applying a constant voltage ($\approx$5 V) to the sample and measuring the current through it using a Keithley 614 electrometer. The measurements were done at room temperature. Electrical contacts were made by applying silver paste over the surface of the films with a separation of 3 mm.

3. Results and discussion

3.1 Structural properties

The crystalline structure of un-doped SnO_2 and SnO_2:Sb films is shown in Fig. 1. The X-ray diffraction patterns of as-deposited films are plotted in Fig. 1 (a). All the patterns show the amorphous structure with some peaks (020), (111), (220) of SnO. Moreover at low Sb-ratio, the peaks of (111) and (042) of Sb_2O_4 and Sb_2O_3, respectively can be observed. Fig. 1 (b) represents the X-ray diffraction of $SnO2_{100-x}Sb_x$ (x =, 3 wt%) films annealed at 300 and 450 ^{o}C.
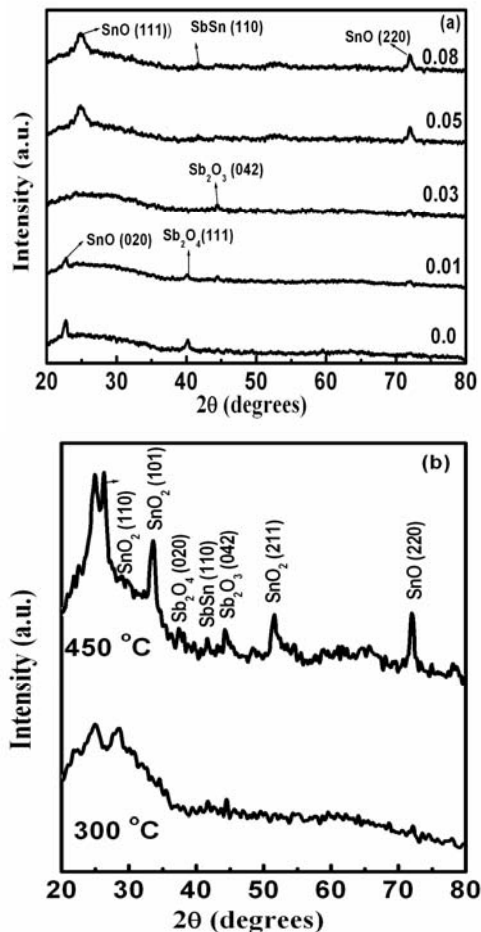

Fig. 1. X-ray diffraction of (a) as-deposited $(SnO_2)_{100-x}Sb_x$ (x =,0, 1, 3, 5, 8 wt%) films and (b) annealed $(SnO_2)_{100-x}Sb_x$ (x =, 3 wt%) films at 300 and 450 ^{o}C.

From this figures it can be observed that, the annealed film at 300 ^{o}C shows the peaks (042) of Sb_2O_3 and (111), (220) of SnO. With increasing the annealing temperature up to 450 ^{o}C, the films show an amorphous matrix containing small randomly oriented crystals. Since the peaks (110), (101), (211) of SnO_2 are observed with intensities higher than those of SnO, Sb_2O_3 and SbSn peaks.

3.2 Optical properties of as-deposited films

The optical transmittance for as-deposited SnO_2:Sb films in wavelength range 200-2500 nm is shown in Fig. 2. From the figure, it is seen that, the transmittance increases with increasing the Sb-content up to x=5 and then starts to decrease with further increase in Sb-content. The maximum transmittance value is approximately 73 % in the visible region of x=0.05.
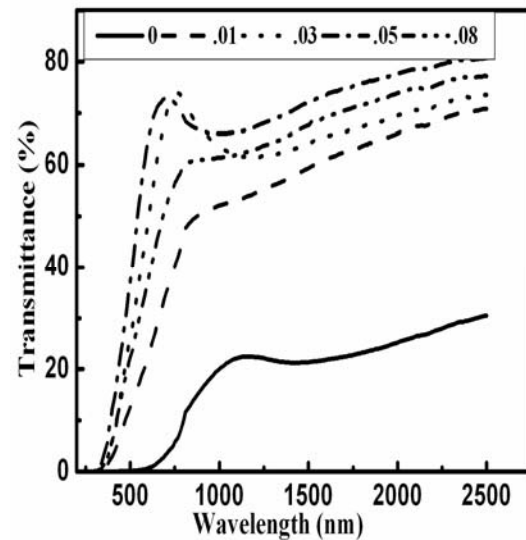

Fig. 2. Transmittance spectra (T %) of as-deposited $SnO2_{100-x}Sb_x$ (x = 0, 1, 3, 5, and 8 wt%) films.

The transmittance of pure SnO_2 films is significantly low, and this may be due to the lack of oxygen resulting during the electron beam evaporation process. This result agrees with that in ref [22]. In order to estimate the optical band gap energy of as-deposited films, the absorption coefficient (α) was calculated using the measured transmittance and reflectance spectra [23]. Then, the optical energy gap (E_g) was obtained by extrapolating the linear region of $\alpha h\gamma$ according to the following relation [24]:

$$\alpha h\gamma = A\left(h\gamma - E_g\right)^n \qquad (1)$$

where A is a constant, $h\gamma$ is the photon energy and n is the factor depend on the nature of electronic transition. The films prepared in the present study have direct allowed transition ($n = 1/2$) as shown in Fig. 3 (a). The values of

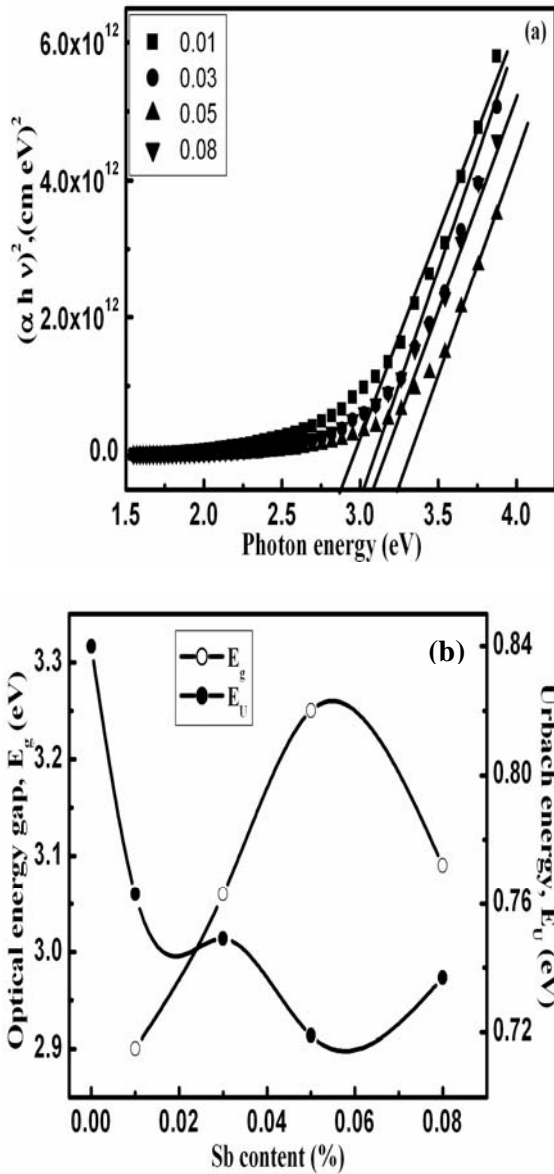optical energy gap was plotted as a function of Sb-content as shown in Fig. 3 (b).

$$\alpha = \alpha_0 \exp\left({h\gamma}/{E_U}\right) \quad (2)$$

Fig. 3. (a) (αhν)² as a function of photon energy and (b) the calculated optical energy gap and Urbach energy of as-deposited SnO2$_{100-x}$Sb$_x$ (x = 0, 1, 3, 5, and 8 wt%) films.

It is observable that, in general, E_g increases with increasing the Sb-content. The increase in the energy gap can be correlated with the Burstein shift. Since the absorption edge of the films shifts to shorter wavelength as shown in Fig. 2. A similar result was noted by X. Feng et al, when they prepared SnO$_2$:Sb films on α-Al$_2$O$_3$ (0001) substrates by MOCVD [25]. Besides, the width of localized states distribution can be determined from Urbach energy (E_U) according to the following equation [26]:

where α_0 is a constant and E_U is the Urbach energy. The values of E_U were calculated and plotted in Fig. 3 (b). From this figure, it is clear that, the Urbach energy has an opposite behaviour of energy gap. This may be due to the decrease in the film disordering with increasing Sb-content as shown in Fig. 1 (a).

The optical free carrier concentration (N) was calculated from the relation of real dielectric constant (ε') according to the following equation [16]:

$$\varepsilon' = n^2 - k^2 = \varepsilon_\infty - \frac{e^2}{4\pi^2 c^2 \varepsilon_0}\left(\frac{N}{m^*}\right)\lambda^2 \quad (3)$$

where n is the refractive index, k is the extinction coefficient, ε_∞ is the high frequency permittivity, e is the electron charge, c is the light velocity, ε_0 is the permittivity of free space, m^* is the effective mass ($m^* = 0.26\ m_0$ [27])and λ is the incident wavelength. The obtained values of N were plotted in Fig. 4. It is clear that, the free carrier concentration decreases with increasing the value of Sb-content. Since, the un-doped SnO$_2$ represents the maximum free carrier concentration value of 2.3×10^{20} cm^{-3}. At high concentration of Sb (x=0.8), the free carrier starts to increase. The decrease in N can be explained due to the appearance of Sb$_2$O$_3$ (Sb^{+3}) in X-ray diffraction as shown in Fig. 1 (a). Since, Sb^{+3} acts as an acceptor which accept the free electrons from the conduction band. In addition, the plasma frequency ω_P is directly proportion to the free carrier concentration as shown from the same figure (Fig. 4).
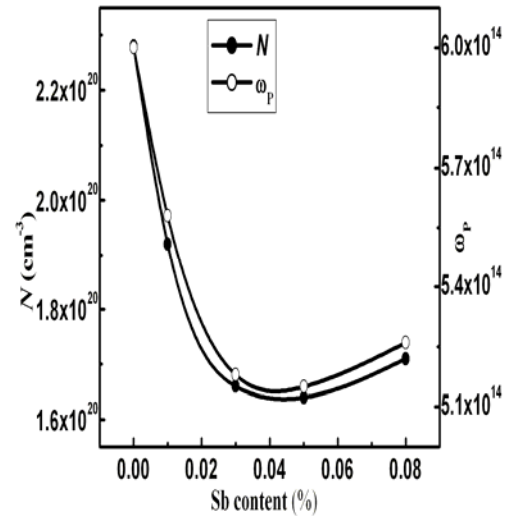

Fig. 4. Variation of free carrier concentration (N) and plasma frequency (ω$_P$)with Sb-content of as-deposited SnO2$_{100-x}$Sb$_x$ (x = 0, 1, 3, 5, and 8 wt%) films.

The values of plasma frequency were determined from the equation [16]:

$$\omega_P = \left(\frac{N e^2}{\varepsilon_0 \, \varepsilon_\infty \, m^*} \right)^{1/2} \qquad (4)$$

The other optical parameters namely; refractive index and extinction coefficient were determined from the optical measurements in the visible region and listed in Table 1. The decreasing in k values with increasing Sb-content is expected therefore the transmittance increased with Sb-content. On the other hand, the refractive index initially decreases with increasing Sb-content and then starts to increase with further increase in Sb-content. This may be due to the behaviour of packing density as explained in ref.28.

3.3 Electrical properties of as-deposited films

Results of the electrical resistivity (ρ)measured at room temperature as a function of Sb-content of as-deposited films are listed in Table 1.

Table 1. Electrical resistivity (ρ) at room temperature, extinction coefficient in the visible region (k_{VIS}) and refractive index in the visible region (n_{VIS}) of as-deposited $SnO2_{100-x}Sb_x$ films of different Sb- contents.

x	0.0	1	3	5	8
ρ (Ω cm)	0.12	1.1×10^3	3.2×10^3	4.4×10^3	4.6×10^3
k_{VIS}	2.12	0.74	0.72	0.32	0.53
n_{VIS}	4.4	3.13	2.91	3.12	3.9

The present films are resistive a matter that can be attributed to their higher degree of amorphization and the decrease in free carrier concentrations with increasing Sb-content as shown in Figs. 1 (a) and 4, respectively. The relatively low resistivity (12×10^{-2} Ω cm) observed for the un-doped films is attributed to the deviation from stoichiometry due to oxygen vacancies [29. 30], which act as electron donors and increase of the free carrier concentration (see Fig. 5).

3.4 Optical and electrical properties of annealed films

To enhance the optical and electrical properties of as-deposited SnO2:Sb films, the effect of heat treatment (annealing) was taken into account. The present study sheds light upon $SnO2_{100-x}Sb_x$ films of x=3 that exhibit the optimal optoelectronic properties as will seen in Fig. 6.

Fig. 5. shows the dependence of both electrical resistivity (ρ) and free carrier concentration (N) upon annealing temperature. It is clear that, the resistivity decreases with increasing annealing temperature up to 400 ^{o}C reaching its minimum value of 6.6×10^{-3} Ω cm. Further increase of annealing temperature resulted in a significant increase of resistivity. On the other hand, the carrier concentrations of theses films behave in reverse way of the resistivity. Therefore, the slight increase in carrier concentrations upon annealing (0-400 ^{o}C) may be attributed to two factors i) the oxygen desorption process. Since, the desorbed oxygen would leave the free electrons behind in the film, leading to increasing of free carrier concentrations. ii) the oxidizing of the films particular the annealing process was done in the air. Beside, the abrupt decrease in carrier concentration that was observed for annealed films above temperature 400 ^{o}C may be due to the chemisorbed oxygen and the formation of grain boundaries acting as trap sites for free electrons. Kim et al [31] and Shanthi et al [32] obtained a similar results.
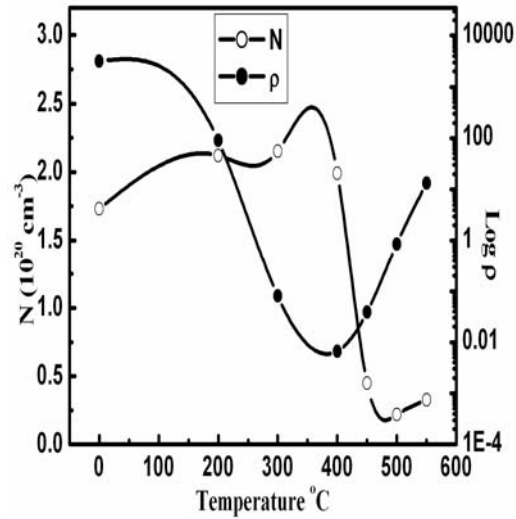

Fig. 5. Variations of free carrier concentrations (N) and electrical resistivity (ρ) with temperature of as-deposited and annealed $SnO2_{100-x}Sb_x$ films of x=3.

Fig. 6 (a) shows the transmittance at wavelength 550 nm as a function of temperature of $SnO2_{100-x}Sb_x$ (x = 0, 1, 3, 5, and 8 wt%) films. It is observed that, with increase the temperature up to 400 ^{o}C the transmittance decrease for all films with different Sb ratios. Beside, the maximum value of transmittance does not exceed 50 % for the films of x=0.05. A significant enhancement of transmittance is observed above temperature 400 ^{o}C. Thus, the transmittance exceeds 84 at 600 nm for $(SnO_2)_{100-x}Sb_x$ films of x=3. The decrease in transmittance upon annealing in the temperature range from as-deposited to 400 ^{o}C may be due to the increase in surface roughness. Therefore, the surface mobility of constituent elements increases and growth of face grains are preferred and degree of surface roughness increases due to heating. Other workers obtained similar results [16, 33, 34]. Beside, the increase in free carrier concentration upon annealing up to 400 ^{o}C as shown in Fig. 5 leads to increase of the free carrier absorption and hence degrades the transparency of these films [35, 36]. On the other hand, the significant increase in transmittance at high temperature is expected to be due to increase the optical energy gap resulting from the improvement of the film ordering as explained by x-ray analysis as shown in Fig. 1 (b). The data of optical energy gap and Urbach energy, for $(SnO_2)_{100-x}Sb_x$ films of x=3, listed in Table 2 confirm our

above discussion. Fig. 6 (b). represents the transmittance spectra of as-deposited and annealed $(SnO_2)_{100-x}Sb_x$ films of x=3. This figure shows a similar behaviour to Fig. 6 (a). The corresponding optical energy gap of these films were calculated and listed in Table 2. Although, the transmittance decreases upon annealing in the temperature range from as-deposited to 400 °C, the energy gap increases. This increase in energy gap may be due to Burstein-Moss effect [37, 38], particularly, the free carrier concentrations increased in this temperature range. At high temperature (> 400 °C), both the transmittance and energy gap increase.
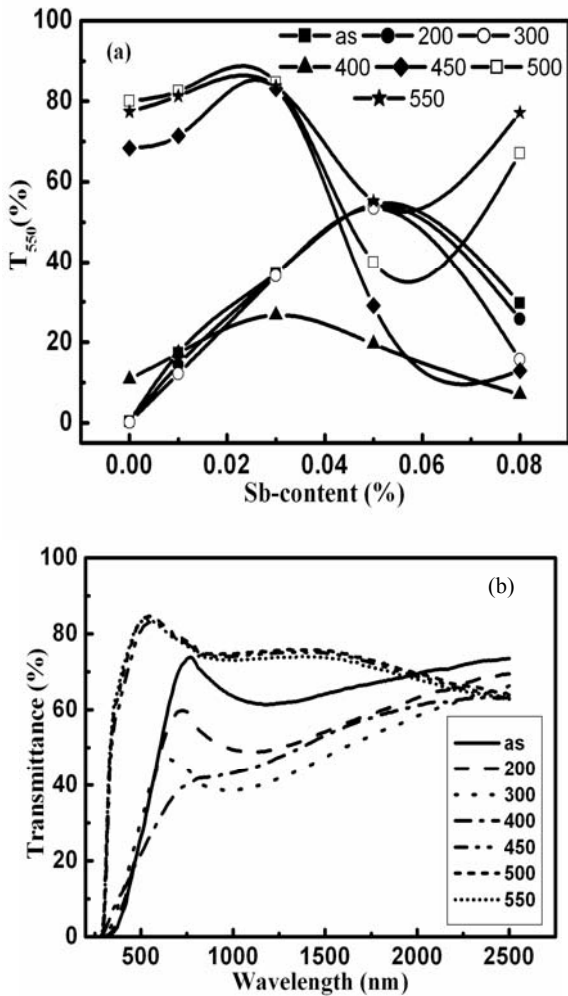
Table 2. Variation of refractive index in the visible region (n_{VIS}), optical energy gap (E_g) and Urbach energy (E_U) with temperature of $(SnO_2)_{100-x}Sb_x$ (x = 3 wt%) films.

T °C	n_{VIS}	E_g (eV)	E_U (eV)
0	2.91	3.06	0.749
200	2	3.07	0.702
300	1.96	3.12	-
400	1.73	2.79	-
450	2.15	3.44	0.631
500	2.11	3.54	0.628
550	2.12	3.52	0.602

Fig. 6. Transmittance spectra a) at wavelength 550 nm (T_{550}) as a function of Sb-content of as-deposited and annealed $SnO2_{100-x}Sb_x$ (x = 0, 1, 3, 5, and 8 wt%) films and (b) of as-deposited and annealed $(SnO_2)_{100-x}Sb_x$ films of x=3 in the wavelength range from 200 to 2500 nm.

Fig. 7 represents the variations in refractive index (n) of the as-deposited and annealed $(SnO_2)_{100-x}Sb_x$ films (x=3) with wavelength. The average refractive index values in the visible region (n_{VIS}) were calculated and listed in Table 2.

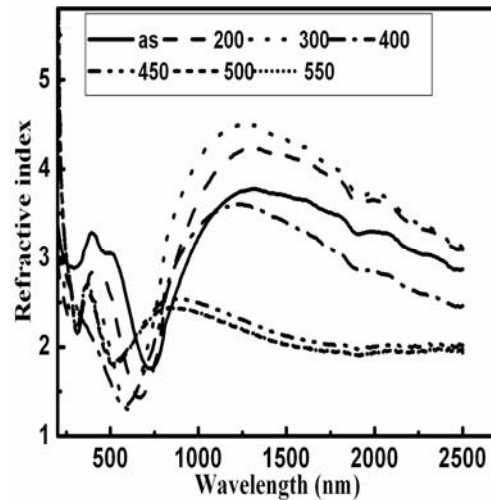*Fig. 7. Variation of refractive index with wavelength of as-deposited and annealed $SnO2_{100-x}Sb_x$ films of x=3.*

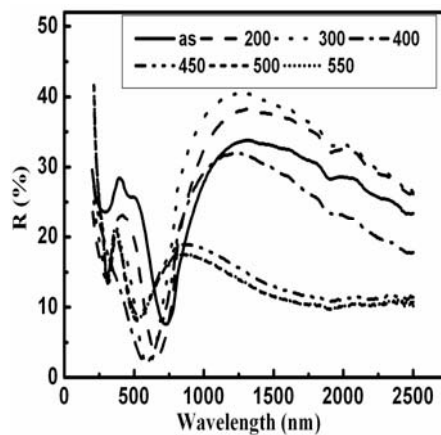*Fig. 8. Reflection spectra (R %) of as-deposited and annealed $SnO2_{100-x}Sb_x$ films of x=3 in the wavelength range from 200 to 2500 nm.*

It is clear that, the refractive index decreases with annealing temperature up to 400 °C and then starts to increase with further increase in the temperature. It is known that [23, 39] the behaviour of refractive index is due to reflection (R %). Therefore, the dependence of reflection on wavelength at different temperatures is shown in Fig. 8.

4. Conclusions

The e-beam evaporation technique was used to prepare transparent conducting SnO_2:Sb films. The effect of Sb-content and annealing temperature was taken into consideration. The as-deposited un-doped SnO_2 films showed low transmittance and low electrical resistivity associated with amorphous structure. With increasing the Sb-content, both the transmittance and resistivity increase. The $(SnO_2)_{100-x}Sb_x$ films of x=3 were selected to study the effect of annealing temperature. It was found that, the transmittance at wavelength 550 nm was significantly increased up to 84 % at temperature 450 ^oC and these films represented direct allowed transition with optical gap 3.06 to 3.54 eV. The temperature above 400 ^oC was sufficient to enhance the structure of these films. The low resistivity of 6×10^{-3} Ω was recorded at the same temperature. It was found that, the refractive index, extinction coefficient, free carrier concentrations, plasma frequency and Urbach energy are very sensitive to Sb-content and annealing temperature. The optimized low resistivity at room temperature and high transmittance at wavelength 550 nm, as well as chemically stable up to high temperatures for the present films, may suggest their suitability for many applications in the field of optoelectronic technology.

References

[1] R. B. H. Tahar, T. Ban, Y. Ohya, Y. Takahashi, J. Appl. Phys. **83,** 2631 (1998).

[2] S. Shanthi, C. Subramanian, P. Ramasamy, J. Cryst. Growth **197**, 858 (1999).

[3] R. Dolbec, M. A. El Khakani, A. M. Serventi, M. C. Horrillo, M. Trudeau, R. G. Saint-Jacques, D. G. Rickerby, I. Sayago, Thin Solid Films **419**, 230 (2002).

[4] F. Arefi-Khonsari, N. Bauduin, F. Donsanti, Thin Solid Films **427,** 208 (2003).

[5] E. Dien, J. M. Laurent, A. Smith, J. Eur. Ceram. Soc. **19**, 787 (1999).

[6] F. J. Yusta, M. L. Hichman, H. Shamlian, J. Mater. Chem. **7**(8), 1421 (1997).

[7] H. N. Wanka, M. B. Schubert, E. Lotter, Sol. Energy Mater. Sol. Cells **41,** 519 (1996).

[8] K. Imamori, A. Masuda, H. Matsumura, Thin Solids Films **395**, 147 (2001).

[9] H. Hosono, H. Ohta, M. Orita, K. Ueda, M. Hirano, Vacuum **66,** (4192002).

[10] B. H. Lee, I. G. Kim, S. W. Cho, S. H. Lee, Thin Solid Films **302**, 25 (1997).

[11] T. Kawashima, T. Ezure, K. Okada Matsui, H. G. Goto, N. Tanabe, J. Photochem. Photobiol. A Chemistry **164,** 199 (2004).

[12] X. Feng, J. Ma, F. Yang, F. Ji, F. Zong, C. Luan, H. Ma, Applied Surface Science **254**, 6601 (2008).

[13] H. Kima, A. Pique, Appl. Phys. Lett. **84**, 218 (2004).

[14] K. S. Kim, S. Y. Yoon,W. J. Lee, K. H. Kim, Surf. Coat. Technol. **138**, 229 (2001).

[15] F. Morazzoni, C. Canevali, N. Chiodini, C. Mari, R. Ruffo, R. Scotti, L. Armelao, E. Tondello, L. Depero, E. Bontempi, Mater. Sci. Eng. C **15,** 167 (2001).

[16] I. Saadeddin , B. Pecquenard , J. P. Manaud , R. Decourta, C. Labruge`re ,T. Buffeteau, G. Campet, Applied Surface Science **253,** 5240 (2007).

[17] P. G. Orsini, P. Pernice, L. Egiziano, J. Electrochem. Soc. **128**, 1451 (1981).

[18] P. H. Duvineaud, D. Reinhard, Sci. Ceram. **12**, 287 (1984).

[19] U. zum Felde, M. Haase, H. Weller, J. Phys. Chem. B **104**, 9388 (2000).

[20] G. Jain, R. Kumae, Opt. Mater. **26**(1), 27 (2004).

[21] Daoli Zhang, Liang Tao, Zhibing Deng, Jianbing Zhang, Liangyan Chen, Materials Chemistry and Physics **100**, 275 (2006).

[22] K. L. Shopra, S. Major, D. K. Panday Thin Solid Films **102,** 1 (1983).

[23] H. A. Mohamed, J. Phys D: Appl. Phys. **40,** 4234 (2007).

[24] B. Stjerna, E. Olsson, C. G. Granqvist, J. Appl. Phys. **78**, 3797 (1994).

[25] X. Feng, J. Ma, F. Yang, F. Ji, F. Zong, C. Luan, H. Ma, Materials Letters **62**, 1779 (2008).

[26] Y. Chang, C. H . Grein, S. Sivananthan, M. E. Flatte, V. Nathan, S. Guha, Appl. Phys. Let. **89**, 1 (2006).

[27] Y. Mi, H. Odaka, S. Iwata, Jpn. J. Appl. Phys. **38**, 3453 (1999).

[28] H. A. Mohamed, H. M. Ali, Sci. Technol. Adv. Mater. **9,** 1 (2008).

[29] A. F. Carroll, L. H. Slack, J. Electrochem. Soc. **123,** 1889 (1976).

[30] I. S. Mulla, A. S. Soni, V. J. Rao, A. P. Sinha, J. Matter. Sci. **21,** 1280 (1986).

[31] I. H. Kim, J. H. Ko, D. Kim, K. S. Lee, T. S. Lee, J.-H. Jeong, B. Cheong, Y.-J. Baik, W. M. Kim, Thin Solid Films **515,** 2475 (2006).

[32] E. Shanthi, A. Banerjee, V. Dutta, K. L. Chopra, Thin Solid Films **71,** 237 (1980).

[33] J. B. Yadav, R. B. Patil, R. K. Puri, Vijaya Puri, Materials Science and Engineering B **139,** 69 (2007) .

[34] P. Rajaram, Y. C. Goswami, D. Rajagopalan, V. K. Gupta, Mater. Lett. **54**, 163 (2002).

[35] H. Kim, J. Horwitz,W. Kim, A. Makinen, Z. Kafafi, D. Chrisey, Thin Solid Films **420–421**, 539 (2002).

[36] H. M. Ali, H. A. Mohamed, M. M. Wakkad, M. F. Hasaneen, Thin Solid Films **515**, 3024 (2007).

[37] E. Burstein, Phys. Rev. **93**, 632 (1954).

[38] T. S. Moss, Proc. Phys. Soc. Lond. Sect. B **67,** 775 (1954).

[39] P. P. Sahay, S. Tewari, K. Nath, Cryst. Res. Technol. **42**, 723 (2007).

[*]Corresponding author: hussein_abdelhafez@yahoo.com